Using the Atomic Force Microscope to Study the Interaction between Two Solid Supported Lipid Bilayers and the Influence of Synapsin I

Ioana Pera,* Rüdiger Stark,* Michael Kappl,* Hans-Jürgen Butt,* and Fabio Benfenati†
*Max-Planck-Institute for Polymer Research, D-55128 Mainz, Germany; and †Department of Experimental Medicine, Section of Human Physiology, University of Genoa, 16132 Genoa, Italy

ABSTRACT To measure the interaction between two lipid bilayers with an atomic force microscope one solid supported bilayer was formed on a planar surface by spontaneous vesicle fusion. To spontaneously adsorb lipid bilayers also on the atomic force microscope tip, the tips were first coated with gold and a monolayer of mercapto undecanol. Calculations indicate that long-chain hydroxyl terminated alkyl thiols tend to enhance spontaneous vesicle fusion because of an increased van der Waals attraction as compared to short-chain thiols. Interactions measured between dioleoylphosphatidylcholine, dioleoylphosphatidylserine, and dioleoyloxypropyl trimethylammonium chloride showed the electrostatic double-layer force plus a shorter-range repulsion which decayed exponentially with a decay length of 0.7 nm for dioleoylphosphatidylcholine, 1.2 nm for dioleoylphosphatidylserine, and 0.8 nm for dioleoyloxypropyl trimethylammonium chloride. The salt concentration drastically changed the interaction between dioleoyloxypropyl trimethylammonium chloride bilayers. As an example for the influence of proteins on bilayer-bilayer interaction, the influence of the synaptic vesicle-associated, phospholipid binding protein synapsin I was studied. Synapsin I increased membrane stability so that the bilayers could not be penetrated with the tip.

INTRODUCTION

The interactions between lipid bilayers have been studied for the past thirty years, with different methods and under various conditions (LeNeveu et al., 1977; Nir and Andersen, 1977; Lis et al., 1982; Marra and Israelachvili, 1985; Persson and Bergenstrahl, 1985; Israelachvili and Wennerström, 1992; McIntosh et al., 1995). The motivation comes from two directions, one biological and one physico-chemical. From the biological point of view, knowledge about the interaction between membranes is essential to understand processes such as exo- and endocytosis, intracellular trafficking, cell division, adhesion, fusion, and metastasis. From the physico-chemical point of view, lipid bilayers are one possible stable phase, namely a lamellar phase, adopted by amphiphilic molecules in aqueous medium. Questions related to the properties of membranes, the internal organization of a bilayer, the understanding of vesicle fusion by rupturing the bilayers, and the forces governing this interaction may be investigated. By clarifying this latter aspect, a quantitative answer to some of the biological questions may be obtained.

Several forces governing bilayer-bilayer interactions have been identified (Israelachvili and Wennerström, 1992). The van der Waals force is long range, attractive, and relatively weak. It is opposed by a short-range repulsive force. This repulsive force decays exponentially with a typical decay length of 0.2–0.5 nm. It is not yet clear which effect dominates this short-range repulsion: the hydration pressure, arising from ordering of water molecules by the hydrophilic head groups of the lipids, or an entropic ''protrusion'' effect of molecular groups that are thermally excited to protrude from the fluid-like lipid bilayers. Charged lipids repel each other by electrostatic double-layer forces. For bilayers, which are not supported on a solid surface, an undulation or fluctuation pressure, due to thermally driven undulations of entire bilayers which couple hydrodynamically to other bilayers keep the surfaces apart.

Several methods have been developed which are capable of determining the forces between two lipid bilayers. In the osmotic stress method (LeNeveu et al., 1976; Parsegian et al., 1979; McDaniel et al., 1983), a suspension of vesicles or oriented multilayers in the lamellar phase is equilibrated with an aqueous solution containing solute such as dextran or polyvinylpyridine. These solutes cannot enter the lipid phase and they compete for water with lipids multilayers, thereby applying an osmotic pressure. The spacing between the multilayers is measured by x-ray diffraction. In this way one obtains pressure-versus-spacing curves. One advantage of the osmotic stress method is that undulation forces can be measured because the lipid bilayers are freely suspended.

An alternative device is the surface forces apparatus. In the surface forces apparatus the force between lipid bilayers supported on two crossed mica cylinders is measured directly (Marra and Israelachvili, 1985; Helm et al., 1989; Benz et al., 2004). In a third method the interaction between two large vesicles formed at the end of micropipettes and imaged by a light microscope is determined (Evans and Metcalfe, 1984). The method is highly sensitive and small pressures can be applied and detected. It also allows determining the mechanical properties of membranes. Since the maximal pressure is given by the Laplace pressure and

Submitted April 13, 2004, and accepted for publication July 8, 2004.

Address reprint requests to Hans-Jürgen Butt, Tel.: 49-6131-379 111; Fax: 149-6131-379 310; E-mail: butt@mpip-mainz.mpg.de.

0006-3495/04/10/2446/10 $2.00

doi: 10.1529/biophysj.104.044214

the size of the vesicles must still be large enough for optical detection, the method is restricted to low repulsive forces.

The atomic force microscope (AFM) has become a major tool to measure forces between surfaces and colloidal particles (Butt, 1991; Ducker et al., 1991). It has also been used to study the interaction between bilayers and silicon nitride or silicon oxide tips (Dufrêne et al., 1998; Mueller et al., 2000; Schneider et al., 2000, 2003; Butt and Franz, 2002; Grant and Tiberg, 2002; Loi et al., 2002; Richter and Brisson, 2003; Künnecke et al., 2004). Therefore solid supported lipid bilayers were formed on a planar surface such as mica or a silicon wafer by Langmuir-Blodgett transfer or spontaneous vesicle fusion. What until now has not been achieved is the reproducible and stable formation of a bilayer on the tip surface.

Here, we report the direct measurement of lipid bilayer interaction by atomic force microscopy. Thus, one bilayer was formed on a planar surface and another one on the AFM tip. The force between these two lipid bilayers was measured versus distance. Both bilayers were formed by spontaneous vesicle fusion. On planar hydrophilic surfaces spontaneous vesicle fusion is a well-known technique to produce homogeneous solid supported bilayers over large areas. More problematic is the reproducible formation of a bilayer on the AFM tip. To adsorb bilayers we coated the AFM tips with a layer of gold and long-chain hydroxyl-terminated alkyl thiols. We demonstrate that the AFM is a reliable tool to assess bilayer-bilayer interactions with respect to other biophysical approaches and that the synaptic vesicle-associated phospholipid binding protein synapsin I has a bilayer stabilizing activity that may function in preserving size and shape of synaptic vesicles and preventing multivesicular fusion.

One advantage of using the AFM is the possibility to image the surface. This is important when studying proteins associated with membranes. We demonstrate this using the protein synapsin I. Synapsin I is a neuron-specific protein specifically associated to synaptic vesicles, the organelles storing and releasing neurotransmitters (De Camilli et al., 1990). Synapsin I has been reported to have an unusually high surface activity and a very large limiting area on amphiphilic surfaces (Ho et al., 1991). Synapsin I binds with high affinity to acidic phospholipids, such as phosphatidylserine or phosphatidylinositol, that are enriched in the cytoplasmic leaflet of the synaptic vesicle membrane (Benfenati et al., 1989a,b). Although the binding of synapsin I involves penetration of the hydrophobic central C domain into the hydrophobic core of the membrane (Benfenati et al., 1989a,b; Stefani et al., 1997), it is not accompanied by either permeabilization or destabilization of the bilayer. Rather, ^{31}P-NMR spectroscopy demonstrated that synapsin I is capable of preventing the transition of PE-containing membrane phospholipids from the bilayer to the inverted hexagonal phase induced by either increases in temperature or addition of Ca^{2+}, thereby increasing the probability for vesicle phospholipids to assume a bilayer organization both under basal conditions and in the presence of destabilizing stimuli such as temperature or Ca^{2+} (Benfenati et al., 1993). Given the high propensity of synapsins to form dimers involving domains distinct from the phospholipid binding domains (Esser et al., 1998; Cheetham et al., 2001), synapsin I is capable to cross-link facing phospholipid membranes, an effect that is believed to promote synaptic vesicle clustering in vivo (Benfenati et al., 1993).

MATERIALS AND METHODS

Dioleoylphosphatidylcholine (DOPC; 1,2-dioleoyl-*sn*-glycero-3-phosphatidylcholine), dioleoylphosphatidylserine (DOPS; 1,2-dioleoyl-*sn*-glycero-3-phospho-L-serine), and dioleoyloxypropyl trimethylammonium chloride (DOTAP; 1,2-dioleoyl-3-trimethylammonium-propane) were purchased from Avanti Polar Lipids (Alabaster, AL). Providers of the other materials were Merck (Darmstadt, Germany; chloroform, potassium chloride, potassium hydroxide), Fluka (Neu-Ulm, Germany; sodium chloride), and Plano GmbH (Wetzlar, Germany; muscovite mica). All chemicals were of analytical grade and were used without further treatment. Synapsin I was purified to homogeneity from calf brain under nondenaturing conditions as previously described (Bähler and Greengard, 1987). Measurements were carried out with a commercial AFM (NanoScope 3, Veeco Instruments, Santa Barbara, CA) using V-shaped silicon nitride cantilevers (Veeco, length 100 μm, width 40 μm, thickness 0.6 μm). Tip radii of curvature R were measured by imaging a silicon grating (TGT01, Mikromasch, Oelsnitz, Germany) and by imaging tips with a scanning electron microscope LEO EM1530 to be between 50 and 70 nm, with few larger tips of up to $R = 250$ nm. In some cases tips even had a parabolic shape at the end. Cantilever spring constants were individually determined by analyzing thermal noise. The majority of spring constants were in the range of 0.2–0.35 N/m. In special cases stiff cantilevers ($\approx$2 N/m) were used.

To coat tips with gold, chips onto which cantilever and tips are mounted were inserted in the evaporation chamber of a Baltec MED 020. First the tips were glow discharged for 120 seconds at a pressure of $\approx$0.02 mbar in air. Afterwards, a 2 nm-thick layer of chromium and a 10 nm-thick layer of gold was evaporated onto the tip at a pressure of 5×10^{-5} mbar. They were allowed to cool under vacuum and then immediately immersed in ethanol solutions containing 1 mM ω-hydroxy-terminated thiols (11-mercapto-undecanol or 2-mercapto-ethanol) for 10–15 h. They were stored in ethanol until needed.

Lipid vesicles for adsorption on mica were prepared as follows: the lipid was first dissolved in chloroform. Then the solvent was evaporated under vacuum. A buffer solution of 150 mM NaCl and 5 mM KH_2PO_4 (titrated to pH 7.4 with KOH) was added to the lipid to produce a 5 mg/mL suspension which was thoroughly sonicated (G112SP1T sonicator, Laboratory Supplies Co., Hicksville, NY) until the suspension became opalescent. Mica was freshly cleaved and mounted onto the AFM scanner. Immediately after cleavage a drop of buffer solution was placed on the mica. Then, the AFM head with liquid cell (volume 40 μL), O-ring, and tip was mounted. Subsequently 50 μL of 50°C warm vesicle solution was pipetted into the cell. After 30 min adsorption time, the cell was rinsed with 1 mL buffer solution to remove vesicles that did not adsorb to the surface. Ten minutes later the measurement started. For control purposes, an image of the lipid bilayer was taken before each measurement to check the bilayer quality. In all measurements, a completely uniform and homogeneous image was obtained.

In a force measurement, the surface was periodically moved up and down at constant speed of 80 nm/s–400 nm/s by applying a voltage to the piezoelectric scanner. An optical detection system, consisting of a laser beam, which is focused onto the back of the cantilever toward a split photodiode, monitored the deflection of the cantilever by forces between the tip and the surface. The result of such a measurement was a curve of

cantilever deflection-versus-height position of the scanner. From this, a force-versus-distance curve, briefly called ''force curve,'' was calculated by multiplying the cantilever deflection by the spring constant to obtain the force, and subtracting the cantilever deflection from the height position to obtain the distance. Experiments were done at 23°C.

RESULTS AND DISCUSSION

Bare silicon nitride tip on mica surface

Before vesicle injection images of mica were flat and showed no adsorbed material. After vesicle adsorption times longer than 30 min, flat surfaces were again observed with the AFM. The presence of a bilayer after vesicle adsorption was verified by taking force curves at different points on the surfaces. In the presence of a bilayer, a characteristic instability and a jump of ~4 nm have been observed after applying a certain load of typically 2–10 nN. This is shown in the approaching parts (*filled circles*) of Fig. 1, *A–C*. This instability was interpreted as the formation of a hole in the solid-supported bilayer and the penetration of the tip (Dufrêne et al., 1998; Schneider et al., 2000, 2003; Butt and Franz, 2002; Grant and Tiberg, 2002; Loi et al., 2002; Richter and Brisson, 2003; Künnecke et al., 2004). These holes in the bilayer formed reversibly. When the tip was retracted, the bilayer filled the holes again and a subsequent force curve looked identical to that obtained before bilayer penetration. The same behavior was observed for all three lipids.

Within one experiment, breakthrough forces were relatively constant and only varied by 5–9% from force curve to force curve. However, when breakthrough forces measured with various tips and various bilayers were compared, a typical and significant twofold variation was observed. This phenomenon could be due to slight variations in the surface properties of the tips, as it was shown that the surface chemistry of the tip can drastically change force curves (Dufrêne et al., 1997; Schneider et al., 2003). It might also be due to different tip shapes since not all tips had the same shape, though we were not able to correlate measured force curves with tip shape. In other cases even the gold coating was partially removed at the very end of the tip. When this happened, we did not take the results into account. As a total, ~2/3 of all experiments lead to results as described above. We also like to mention that in some experiments a second jump of short jump distance (1 nm) and at higher forces was observed. We have neither an explanation for it nor can we deliberately produce this jump.

No clear dependence of breakthrough forces F on the tip radius was observed. It is, however, questionable whether breakthrough forces should be proportional to the tip radius R or not. The assumption that F scales with R is based on Derjaguin's law, which says that in equilibrium and if R is much larger than the characteristic decay length of the interaction, the force is proportional to R (Derjaguin, 1934). For the breakthrough the system is not in equilibrium and the rupture of the lipid bilayer might not be proportional to R. This can be illustrated with the simple assumption that the lipid bilayer ruptures if a certain pressure underneath the tip is acceded. Using the elastic foundation model (Johnson, 1985) for a parabolically shaped tip the maximal pressure underneath the tip is

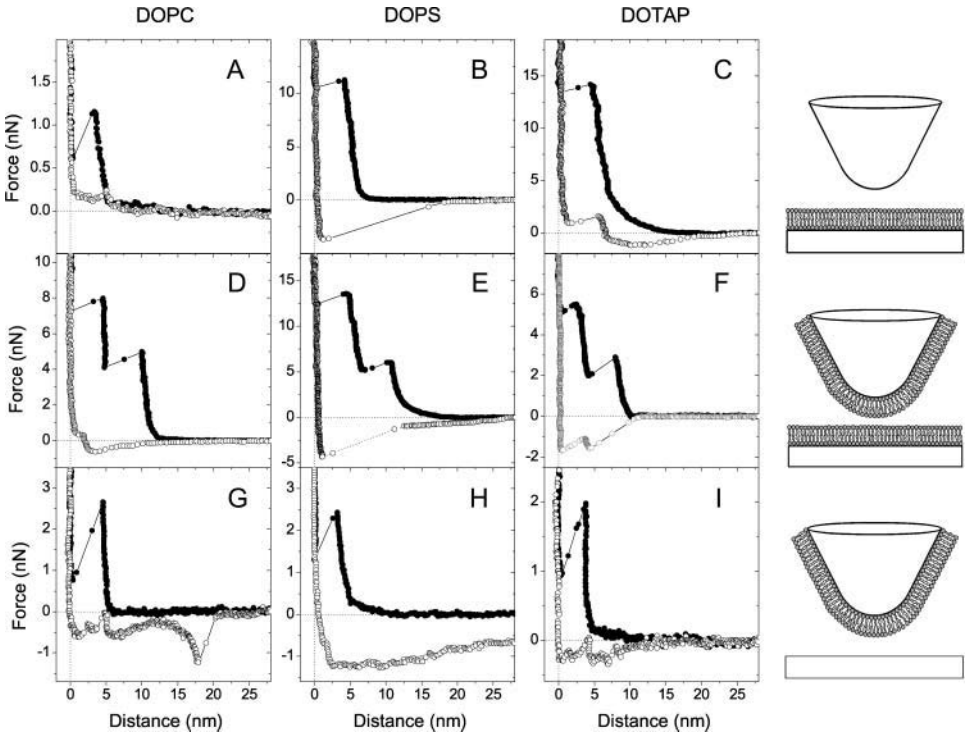

FIGURE 1 Typical force-versus-distance curve measured on a planar mica surface with a bare silicon nitride tip in buffer after exposure to (*A*) DOPC (radius of curvature of the tip $R = 45$–50 nm), (*B*) DOPS ($R = 100$–150 nm), and (*C*) with DOTAP ($R = 200$–250 nm) vesicles. The schematic on the right shows our interpretation of where bilayers are adsorbed. Force curves obtained with a mercapto undecanol ($HS(CH_2)_{11}OH$)-gold coated tip on mica after exposure to (*D*) DOPC ($R = 45$–50 nm), (*E*) DOPS ($R = 100$–120 nm), and (*F*) DOTAP ($R = 100$–120 nm) vesicles. Typical force curves obtained with a mercapto undecanol-gold coated tip on a planar mercapto ethanol ($HS(CH_2)_2OH$)-gold surface after exposure to (*G*) DOPC ($R = 60$–65 nm), (*H*) DOPS (*R* unknown), and (*I*) DOTAP ($R = 70$–75 nm) vesicles.

$$P_{\max} = \sqrt{\frac{EF}{\pi l_0 R}}, \quad (1)$$

where l_0 is the thickness of the bilayer in equilibrium and E is Young's modulus of the bilayer. In this case the breakthrough force scales with $F \propto R^{-1/2}$. For other rupture models, the scaling might be different (Butt and Franz, 2002).

Increasing approaching velocity slightly increased the breakthrough force as has been described experimentally and theoretically earlier (Butt and Franz, 2002; Loi et al., 2002). Within the range of approaching velocities we applied (80–400 nm/s) this increase was, however, below 20%.

Solid supported lipid bilayers also form on silicon nitride (Puu and Gustafson, 1997). In force measurements, however, we usually observed only one jump over a distance corresponding to the thickness of one bilayer. Thus, we found no indication for a bilayer adsorbed to the tip. If there is an adsorbed bilayer, it was only weakly bound so that the force required to remove it was not significant. This was also suggested by Grant and Tiberg (Grant and Tiberg, 2002). One possible reason why bilayers adsorb spontaneously to a planar surface, but not to the tip, is the high curvature. The energy per unit area required to bend a bilayer with zero spontaneous curvature to a spherical cap is $2\kappa/R^2$. Here, κ is the bending rigidity, also called bending elastic modulus. For phosphatidylcholine bilayers in the liquid phase κ is typically 10^{-19} J (Servuss et al., 1976; Sackmann et al., 1986; Evans and Needham, 1987; McIntosh et al., 1995; Petrache et al., 1998). For the spontaneous adsorption of a bilayer, the adsorption energy must be higher than the bending energy. With typical adsorption energies per unit area of $W_A = 0.2–2 \times 10^{-4}$ J/m^2 (Evans and Needham, 1987; Rädler et al., 1995), the minimal radius of curvature is estimated to be $R = \sqrt{2\kappa/W_A} = 100–32$ nm, respectively. Only for a strong adhesion between the bilayer and the solid surface we expect that the tip surface is covered. The stronger the adsorption, the smaller the tip can be. In any case: very sharp tips are not going to be covered by bilayers.

Bare silicon nitride tip, thiol-modified planar gold surfaces

In a different set of experiments planar surfaces were coated with gold and two different thiols: 11-mercapto-undecanol and 2-mercapto-ethanol. After exposing these surfaces to a vesicle suspension we measured again force curves on both surfaces. A jump of 3.5–6 nm was observed on mercapto undecanol. The mean breakthrough force was 6–15 nN. In contrast, no jump could be detected on mercapto ethanol. By choosing a specific thiol, vesicle fusion could be induced or prevented. This is relevant with respect to sensor applications. For sensors of electrochemical reactions at lipid bilayers a conducting surface, such as gold, rather than an insulator, such as mica or glass, is required. That a short-chain thiol did not induce vesicle fusion is in line with results of Sofou and Thomas (2003) and Jenkins et al. (2001) who observed that on gold coated with acetyl cystein and mercapto ethanol vesicles adsorb but usually remain intact. Intact vesicles are probably removed by the AFM tip while scanning.

Why are lipid bilayers stronger attracted by long-chain rather than short-chain thiols? We think that this is due to van der Waals forces. To support this hypothesis we calculate the van der Waals force for a thiol layer on gold interacting with a lipid layer across water. The thickness T of the hydroxyl-terminated alkyl thiol is varied between 0.5 and 2.0 nm; 0.5 nm roughly corresponds to the thickness of a mercapto ethanol monolayer and 1.5 nm to a mercapto undecanol monolayer. The lipid layer (of infinite thickness) being a separation D away from the hydroxyl-terminated alkyl thiol layer represents the vesicle; calculations with a lipid layer of only 4 nm showed no significant difference to an infinitely extended lipid layer. Calculated force per unit area-versus-distance curves show that a lipid layer is repelled from gold with a small T whereas it is attracted at large T (Fig. 2). The reason is that gold has a stronger van der Waals attraction to water than to hydrocarbon. Therefore, if the gold dominates, water is preferred over lipid and the vesicles are repelled. This is the case for a mercapto ethanol layer. If the alcohol layer is thick enough, the influence of the gold is reduced. In this case the van der Waals attraction of the hydroxyl-terminated alkyl thiols across water dominats, leading to a net attraction. Though this model of the van der Waals interaction between a lipid bilayer and a hydroxyl-terminated alkyl thiol on gold is highly simplified, the

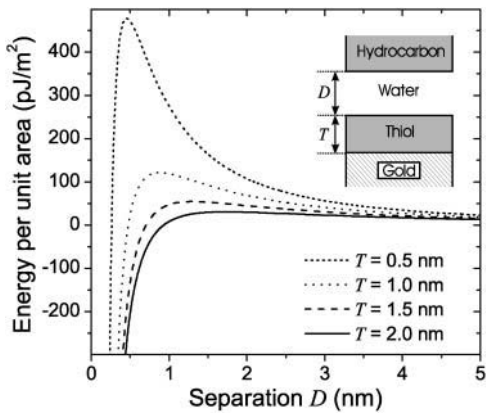

FIGURE 2 Van der Waals force per unit area calculated for gold coated with hydroxyl terminated alkyl layer of thickness T interacting across water with an infinitely thick alkyl layer. It was calculated with Eq. 11.8 of Israelachvili (1992). For the Hamaker constant of thiol/water/lipid, we use a value of 3×10^{-21} J reported for lipid/water/lipid (Israelachvili, 1992). For the Hamaker constant of gold/thiol/gold, we estimate a value of 3×10^{-19} J based on a calculation using Eq. 11.27 of Israelachvili (1992) with Hamaker constants reported for gold/vacuum/gold and for gold/polystyrene/gold (Visser, 1972).

increased van der Waals attraction for long-chain mercapto alcohols explains the observed effect.

Mercapto undecanol-gold coated tip

To adsorb bilayers to the tip, we coated tips with gold and a monolayer of mercapto undecanol. After exposing tip and surface to a vesicle suspension, two jumps were usually observed for all three lipids (approaching parts in Fig. 1, *D–F*). Typical, jump distances were 4 nm. This is a clear indication that a bilayer had adsorbed to the tip in addition to that adsorbed to the surface. Thus, under these conditions, we are able to measure bilayer-bilayer interactions (Table 1).

The repulsion before the first jump could be described by an exponential function. Decay lengths were 0.7 nm for DOPC, 1.2 nm for DOPS, and 0.8 nm for DOTAP. This agrees with the tendency observed here and earlier (Mueller et al., 2000) with bare tips on bilayers with the same lipids. No significant attractive force component was observed. The reason is that under our conditions van der Waals forces are too low to be observed with the AFM. Van der Waals forces between a planar bilayer and a bilayer on a spherical tip can be calculated with $F = -A_{\mathrm{H}}R/(6D^2)$, where A_{H} is the Hamaker constant for lipid interacting with lipid across water and D is the distance between the two bilayer surfaces (not to be confused with the distance in the figures which is the distance between the solid support and the tip surface). With a Hamaker constant of 3×10^{-21} J (Israelachvili, 1994) and a tip radius of 100 nm the van der Waals force is 0.05 nN at a distance of 1 nm. At this distance the exponential repulsive force becomes already dominating.

The observation of two jumps can be interpreted in two ways (Fig. 3). Either one of the bilayers breaks and reversibly forms a hole or two monolayers break (Richter and Brisson, 2003) and the two remaining monolayers fuse to form a new bilayer. Based on the AFM experiments it is not possible to decide which of the two configurations is assumed in reality or if both occur.

Schneider et al. (2000, 2003) coated tips with mercapto hexadecanol and measured forces on mica in solution. They, however, formed their bilayers by the Langmuir-Blodgett technique and not by spontaneous vesicle fusion. For this reason they only observed one jump.

On mercapto ethanol-coated gold surfaces, only single jumps were observed after exposure to vesicle suspensions (approaching parts Fig. 1, *G–I*). In this case, we interpret the jump as a break through the bilayer on the tip, whereas no bilayers are adsorbed to the planar surface. Thus, by choosing the appropriate coating of the surfaces, we can measure bilayer-tip, bilayer-bilayer, and planar surface-bilayer interactions.

Mercapto ethanol-gold coated tip

When the tip was coated with gold and mercapto ethanol, no second jump was detected, which we take as an indication

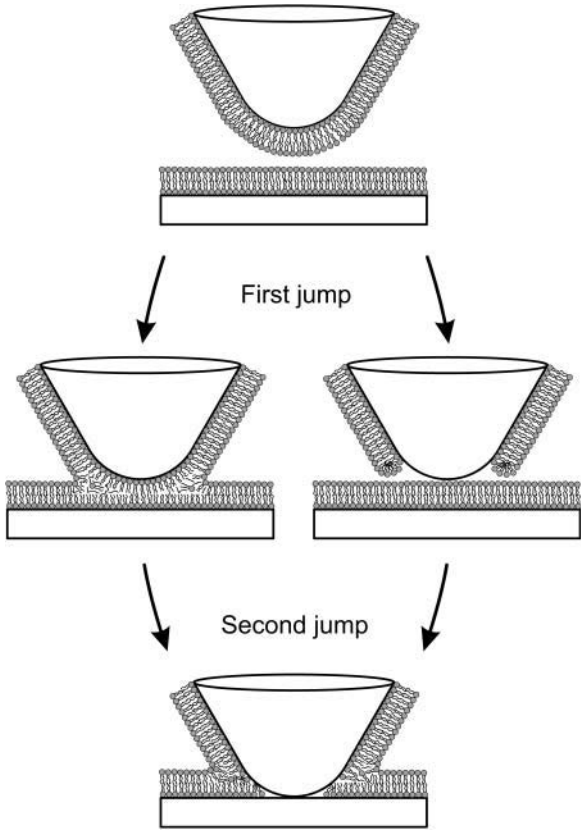

FIGURE 3 Schematic of two possible mechanisms of a bilayer coated tip jumping in two steps through a bilayer coated planar surface.

that no lipid bilayers had formed on the tip; the substrate was mica. In addition, also the breakthrough force for the remaining jump was reduced to 0.5–4 nN. This can be understood based on the nucleation theory for tip-induced film rupture (Butt and Franz, 2002; Loi et al., 2002). Qualitatively, the rupture of the lipid bilayer and the formation of a hole through which the AFM tip can penetrate is hindered by the ''spreading pressure'' S. The spreading pressure increases proportional to the adsorption energy of the bilayer to the solid surfaces of the tip and to the planar surface. For a strong adsorption to the tip surface S should be high, whereas for a weak adsorption it should be low. The adsorption energy on mercapto ethanol is weaker than on bare silicon oxide or silicon nitride. For this reason we expect the breakthrough force to be reduced.

Retracting force curves

Retracting force curves tended to vary from experiment to experiment and are not as reproducible as approaching force curves. In some experiments the retracting force curves even varied from one position to another position and changed with time (typically hours). We present retracting force curves (Fig. 1, *open symbols*), start to categorize certain

features, and propose interpretations. We are, however, not able to relate these features uniquely to certain lipids or tip coatings.

In some cases ''partially reversible'' force curves were observed (e.g., Fig. 1 *A*). There the tip was released from direct contact at a positive force. The bilayer has a strong tendency to coat the surfaces, so that it pushes the tip away from the surface. After being released from direct contact, approaching and retracting force curves are identical. Such reversible force curves were also described by Grant et al. on DOPC bilayers coadsorbed with dodecylmaltoside (Grant and Tiberg, 2002).

In many cases, ''contact adhesion'' was observed (e.g., Fig. 1 *B*). A certain force, the adhesion force, had to be applied to pull the tip off from direct contact with the solid planar surface. Once released, the tip jumps back to the approaching force curve and from that point on the force curve is reversible. When two bilayers are present, contact adhesion can occur twice (Fig. 1 *F*): First the adhesion between tip and planar surface and then the adhesion between one bilayer and the tip. Contact adhesion was observed and analyzed by Schneider et al. (2003) on different lipid bilayers prepared by Langmuir-Blodgett transfer with thiol-coated tips and by Künnecke et al. (2004) with uncoated tips on bilayers prepared by vesicle fusion. Schneider et al. (2003) conclude that adhesion forces can be analyzed in terms of classical theories of contact mechanics such as the JKR theory (Johnson, 1985).

In few cases a ''weak long-range attraction'' was observed in addition to the above mentioned features (Fig. 1, *C* and *E*). It is at least 10 times lower than the breakthrough force and certainly below 1 nN. It does not depend strongly on distance and is sometimes relatively constant until it drops to zero at distances of up to 20 nm. Such weak long-range attraction has been described before (Maeda et al., 2002; Richter and Brisson, 2003). It indicates that some kind of contact is maintained over distances exceeding the thickness of the two bilayers. A possible mechanism leading to the weak long-range attraction is the formation of a bilayer tether between the tip and planar surface (Fig. 4) (Maeda et al., 2002). Such membrane tethers have also been observed on various whole cells by different methods (e.g., Hochmuth et al., 1973; Sheetz, 2001). The force required to extend such a tube is $F \approx 4\pi r\gamma$, where γ is the surface tension of a lipid bilayer and r is the radius of the tube. With $r = 10$ nm and $\gamma = 0.001$ N/m we estimate a force of 0.13 nN. This agrees with what was observed.

In addition, rare features were observed such as a short jump out (jump distance much smaller than the bilayer thickness, e.g., Fig. 1 *D* (Richter and Brisson, 2003) and forces resembling the stretching of single polymer chains (Fig. 1 *G*, see) (Janshoff et al., 2000) or strong long-range attraction (Fig. 1 *H*).

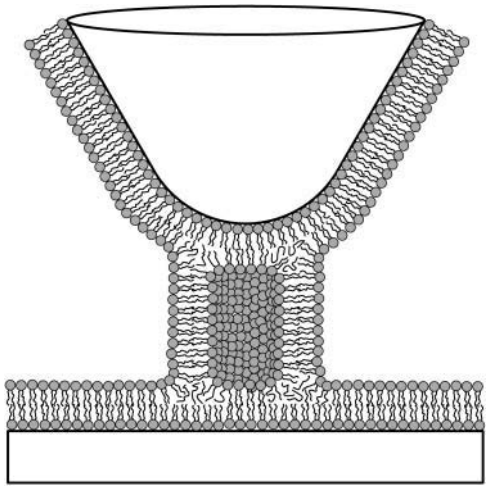

FIGURE 4 Schematic of a bilayer tether formed when the tip is retracted from the planar surface.

Formation of stacks

Stacks of three and in some cases more bilayers could be formed by first incubating the planar surface with DOPS (or DOTAP), rinse with buffer, and mount the AFM cell. Then a vesicle suspension with the oppositely charged DOTAP (DOPS) was added. After typically 30 min, the suspensions was rinsed off by pure buffer and force curves were collected. During the whole procedure, the surfaces were kept in aqueous medium. The resulting force curves show three jumps of ~4 nm each, indicating that indeed a stack of DOPS-DOTAB (DOTAP-DOPS) bilayers had formed on the planar surface, whereas a DOTAP (DOPS) bilayer was on the tip (Fig. 5).

Salt concentration

All results reported so far were obtained in buffer with a relatively high ionic strength of 150 mM. To determine the influence of salt concentration on the bilayer-bilayer interaction, experiments were done with DOTAP in water containing various concentrations of KNO_3. The breakthrough force for the outer jump decreased as the salt concentration was reduced (Fig. 6, *top*). This indicates that the charged bilayer is stabilized by salt. In addition, the long-range electrostatic double-layer force became visible. Its decay length increased with decreasing salt concentration and agreed with the calculated Debye length. At salt concentrations below 3–5 mM, the outer jump disappeared. When increasing the salt concentration the second jump

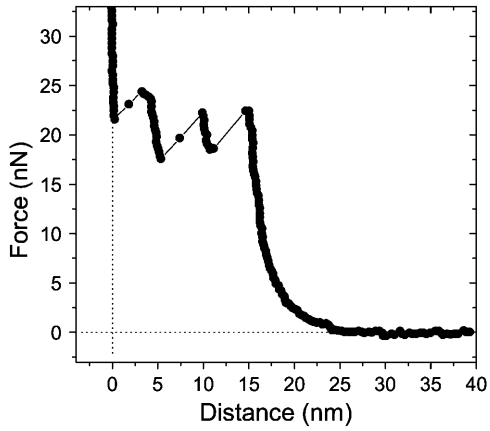

FIGURE 5 Force curve measured on mica preincubated with DOPS after addition of DOTAP in standard buffer (150mM NaCl, 5mM KH_2PO_4, with KOH titrated to pH = 7.4). The tip was coated with mercapto undecanol-gold.

appeared again as before. Even on retraction these two jumps were visible.

When taking *many* force curves at the same spot at intermediate salt concentrations of $c = 5$–10 mM the number of jumps increased to typically five (Fig. 6, *bottom*). Changing back to either low or high salt concentration lead to either one ($c \leq 2$ mM) or two ($c = 150$ mM) jumps. Thus, at intermediate salt concentrations, the tip induced stack formation. In contrast, at high salt or low concentration we did not observe a change in the force curves, even when taking hundreds of force curves at the same spot.

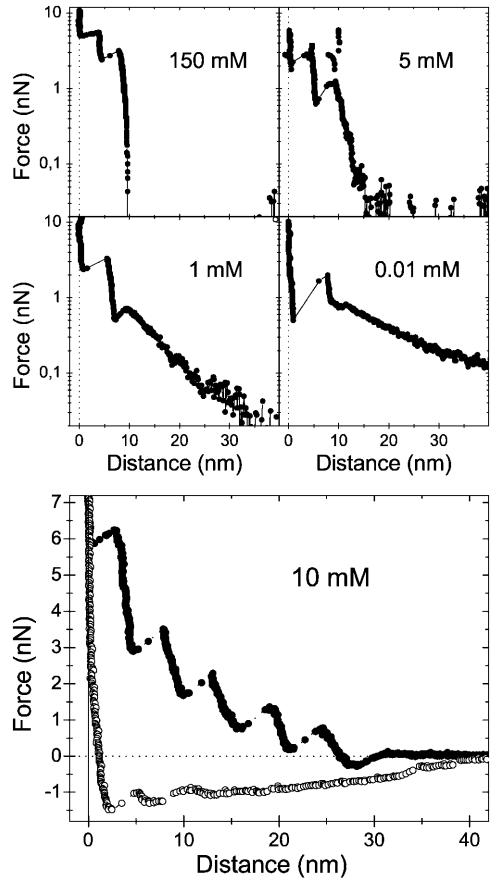

FIGURE 6 (*Top*) Approaching force curves measured at the indicated concentrations of KNO_3 for DOTAP showing the different decay lengths. (*Bottom*) Force curve observed on DOTAP in 10 mM KNO_3 after taking 306 force curves at the same spot. Mercapto undecanthiol-gold-coated tip ($R = 100$–120 nm), mica sample.

Synapsin I

Five minutes after injecting a synapsin I solution at a concentration of 0.5 μg/mL into the fluid cell onto a DOPS bilayer, elevations were observed which became more frequent and larger with time (Fig. 7). These elevations had a defined height of 2.5 nm and can be interpreted as synapsin aggregates of monomolecular thickness attached to the lipid bilayer. Aggregates grew progressively in surface and eventually became confluent and filled the entire area.

Images of synapsin aggregates on lipid bilayers could be recorded both with bare silicon nitride tips and with tips coated with mercapto undecanethiol-gold. In the latter case, a bilayer was present on the tip and the image was taken with a lipid bilayer scanning a bilayer on the planar surface. This ensured a relatively low imaging force, significantly below the first breakthrough force.

Images showing the adsorption (Fig. 7) were recorded in the presence of synapsin in the AFM cell. When the cell was rinsed with pure buffer at a certain time, the adsorption process stopped and the synapsin aggregates stopped growing in size. At this point, force curves could be taken on either synapsin aggregates or on pure bilayers regions (Fig. 8). If a bare silicon nitride tip was used, no jump was observed in synapsin regions, whereas the typical jump was detected in pure bilayer regions. Even close to the rim of synapsin-coated domains, the force curves did not change and were indistinguishable from force curves taken far inside a bilayer region. The maximal force which could be applied was of the order of 23 nN. The data indicate that synapsin I stabilizes the membrane and prevents the tip from penetrating the bilayers.

When a mercapto undecanthiol-gold tip was used, with a bilayer likely present on the tip, two types of force curves were observed in each region (Fig. 9). In synapsin-coated areas, either a single jump (mean breakthrough force at 10–12 nN, jump-distance of 3.5–4.0 nm) or no jump at all was observed. We believe that the jump observed in the former case was due to a rupture of the synapsin-free bilayer present on the tip, whereas the absence of any jump observed in the latter case is attributable to the presence of synapsin at the end of the tip which makes the bilayer relatively stiff. In pure bilayer regions, we observed either a single jump (mean breakthrough force 10–12 nN, jump distance 3.5–4.0 nm) or

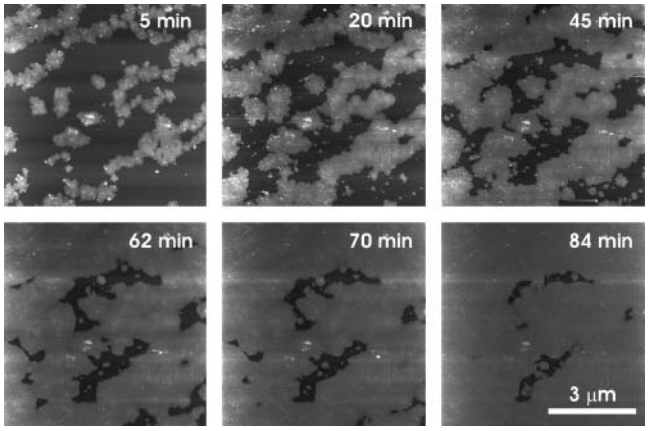

FIGURE 7 Sequence of AFM images of synapsin I adsorption to a DOPS bilayer in 0.2 M NaCl, 1 mM EDTA, 1 mM EGTA, 1 mM 2-mercapto ethanol, 3 mM NaN_3, 25 mM TrisCl, pH 7.5 aqueous solution containing 0.5 μM synapsin I. Images were taken with a mercapto undecanethiol-gold coated tip to which a bilayer was adsorbed, at a force below the outer breakthrough. Light areas are high, dark area low. The total height scale is 7 nm. Images were taken at 5, 20, 45, 62, 70, and 84 min after synapsin injection.

two jumps (mean breakthrough forces at 10–12 nN and 1.5–2.5 nN, jump distances 3.0–3.5 nm and 5.5–6.0 nm). In this case, we believe that the single jump is due to the presence of a synapsin-coated bilayer at the end of the tip, whereas the double jump occurs when a pure lipid bilayer is present at the end of the tip.

By using the AFM technique, we have provided a direct demonstration of the phospholipid bilayer stabilizing activity of synapsin I. This is consistent with the data previously obtained with the analysis of the ^{31}P-NMR powder pattern (Benfenati et al., 1993). The synapsins are amphiphilic

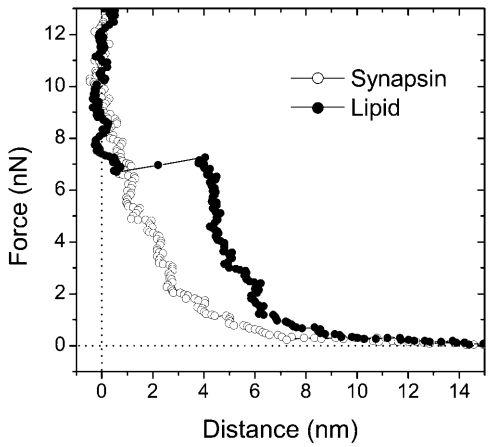

FIGURE 8 Force curves recorded with a bare silicon nitride tip ($R = 60$ nm) on a synapsin-free lipid region (*closed symbols*) and a synapsin-coated region (*open symbols*). The 5 μM synapsin solution in PBS buffer was incubated with the DOPS bilayer for 30 min. For details, see legend to Fig. 7.

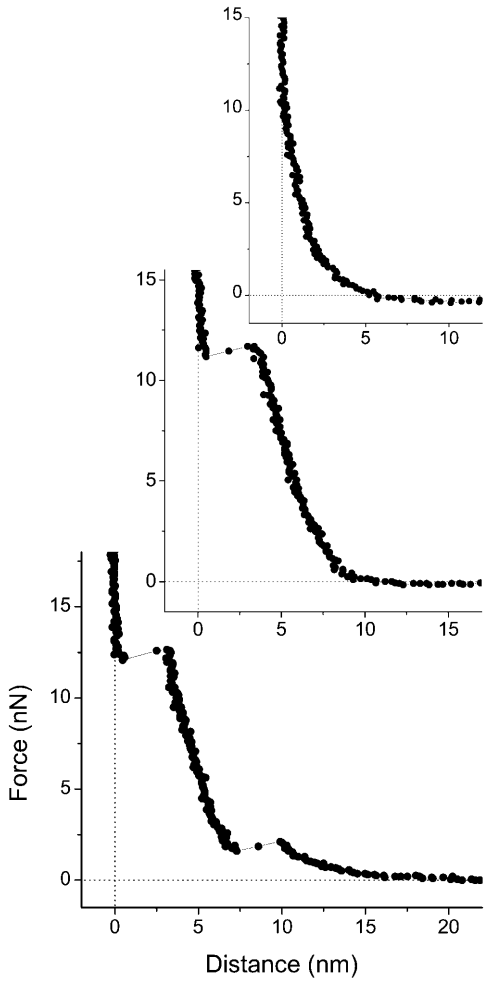

FIGURE 9 Force curves recorded with a tip coated with gold and mercapto dodecanol on mica in the presence of lipid bilayers and synapsin I. Presumably, a layer of lipids either free or coated with synapsin I is present on both the planar surface and the tip. Three types of force curves were observed: (*top*) no jump at all, attributable to the presence of two synapsin-coated bilayers; (*middle*) one jump, attributable to the presence of one synapsin-coated and one pure lipid regions; and (*bottom*) two jumps attributable to the presence of two pure lipid regions. Measurements were done in 0.2 M NaCl, 1mM EDTA, 1 mM EGTA, 3 mM NaN_3, 1 mM 2-mercapto ethanol, 25 mM Tris-HCl, pH 7.5. The surfaces were exposed to DOPC vesicles for 30 min. $R = 125$–150 nm.

proteins specifically associated with the cytoplasmic surface of synaptic vesicles. These vesicles are among the smallest intracellular organelles and their membrane is characterized by a very high curvature and can experience phospholipid packing defects (Hui et al., 1981; Hoekstra, 1982). The high propensity of synapsin I to form a monomolecular layer that covers large phospholipid surfaces shown here supports the possibility that, in nerve terminals, synapsin I covers a large portion of the synaptic vesicle surface (De Camilli et al., 1990; Ho et al., 1991). Furthermore, the ability of synapsin I to stabilize phospholipid bilayers found in this study may be important in the maintenance of the uniform size, regular

TABLE 1 Mean jump distances and breakthrough forces of outer and inner jump as well as the decay length of the exponentially repulsive force before the outer jump for bilayer-bilayer interaction

	DOPC	DOPS	DOTAP
Inner	4.8 nm 8 nN	3.0 nm 9 nN	2.8 nm 11 nN
Outer	5.3 nm 3 nN	3.1 nm 5 nN	5.5 nm 7 nN
Decay length	0.7 nm	1.2 nm	0.8 nm

shape, and structural integrity of synaptic vesicles, as well as in the prevention of random fusion events.

In conclusion, we have shown that the AFM technique with tip-bilayer or bilayer-bilayer conformation is well-suited to study the stability of a solid supported bilayer as well as to characterize bilayer-bilayer interactions. This approach could be useful to investigate the mechanisms of membrane fusion and fission that occur within cells and in neurons during exo-endocytosis and the effects of phospholipid binding proteins on membrane dynamics.

We acknowledge financial support of the German Research Foundation DFG Bu 701/22 (I.P.), the Italian Ministry of University Cofin and FIRB grants, Consorzio Italiano di Biotecnologie, and Fisher Center for Alzheimer's Disease Research (F.B.).

REFERENCES

Bähler, M., and P. Greengard. 1987. Synapsin I bundles F-actin in a phosphorylation-dependent manner. *Nature*. 326:704–707.

Benfenati, F., M. Bähler, R. Jahn, and P. Greengard. 1989a. Interactions of synapsin I with small synaptic vesicles: Distinct sites in synapsin I bind to vesicle phospholipids and vesicle proteins. *J. Cell Biol.* 108:1863–1872.

Benfenati, F., P. Greengard, J. Brunner, and M. Bähler. 1989b. Electrostatic and hydrophobic interactions of synapsin I and synapsin I fragments with phospholipid bilayers. *J. Cell Biol.* 108:1851–1862.

Benfenati, F., F. Valtorta, M. C. Rossi, F. Onofri, T. Sihra, and P. Greengard. 1993. Interactions of synapsin I with phospholipids: Possible role in synaptic vesicle clustering and the maintenance of bilayer structures. *J. Cell Biol.* 123:1845–1855.

Benz, M., T. Gutsmann, N. Chen, R. Tadmor, and J. Israelachvili. 2004. Correlation of AFM and SFA measurements concerning the stability of supported lipid bilayers. *Biophys. J.* 86:870–879.

Butt, H.-J. 1991. Measuring electrostatic, van der Waals, and hydration forces in electrolyte solutions with an atomic force microscope. *Biophys. J.* 60:1438–1444.

Butt, H.-J., and V. Franz. 2002. Rupture of molecular thin films observed in atomic force microscopy. I. Theory. *Phys. Rev. E.* 66:031601.

Cheetham, J. J., S. Hilfiker, F. Benfenati, T. Weber, P. Greengard, and A. J. Czernik. 2001. Identification of synapsin I peptides that insert into lipid membranes. *Biochem. J.* 354:57–66.

De Camilli, P., F. Benfenati, F. Valtorta, and P. Greengard. 1990. The synapsins. *Annu. Rev. Cell Biol.* 6:433–460.

Derjaguin, B. 1934. Untersuchungen über die Reibung und Adhäsion. *Kolloid Z.* 69:155–164.

Ducker, W. A., T. J. Senden, and R. M. Pashley. 1991. Direct measurement of colloidal forces using an atomic force microscope. *Nature*. 353:239–241.

Dufrêne, Y. F., W. R. Barger, J. B. D. Green, and G. U. Lee. 1997. Nanometer-scale surface properties of mixed phospholipid monolayers and bilayers. *Langmuir*. 13:4779–4784.

Dufrêne, Y. F., T. Boland, J. W. Schneider, W. R. Barger, and G. U. Lee. 1998. Characterization of the physical properties of model biomembranes at the nanometer scale with the atomic force microscope. *Faraday Discuss.* 111:79–94.

Esser, L., C. R. Wang, M. Hosaka, C. S. Smagula, T. C. Sudhof, and J. Deisenhofer. 1998. Synapsin I is structurally similar to ATP-utilizing enzymes. *EMBO J.* 17:977–984.

Evans, E., and M. Metcalfe. 1984. Free energy potential for aggregation of giant, neutral lipid bilayer vesicles by van der Waals attraction. *Biophys. J.* 46:423–426.

Evans, E., and D. Needham. 1987. Physical properties of surfactant bilayer membranes: Thermal transitions, elasticity, rigidity, cohesion, and colloidal interactions. *J. Phys. Chem.* 91:4219–4231.

Grant, L. M., and F. Tiberg. 2002. Normal and lateral forces between lipid covered solids in solution: correlation with layer packing and structure. *Biophys. J.* 82:1373–1385.

Helm, C. A., J. N. Israelachvili, and P. M. McGuiggan. 1989. Molecular mechanisms and forces involved in the adhesion and fusion of amphiphilic bilayers. *Science*. 246:919–922.

Ho, M. F., M. Bähler, A. J. Czernik, W. Schiebler, F. J. Kezdy, E. T. Kaiser, and P. Greengard. 1991. Synapsin I is a highly surface-active molecule. *J. Biol. Chem.* 266:5600–5607.

Hochmuth, R. M., N. Mohandas, and P. L. Blackshear. 1973. Measurement of the elastic modulus for red cell membranes using a fluid mechanical technique. *Biophys. J.* 13:747–762.

Hoekstra, D. 1982. Role of lipid phase separations and membrane hydration in phospholipid vesicle fusion. *Biochemistry*. 21:2833–2840.

Hui, S. W., T. P. Stewart, L. T. Boni, and P. L. Yeagle. 1981. Membrane fusion through point defects in bilayers. *Science*. 212:921–923.

Israelachvili, J. N. 1992. Intermolecular and Surface Forces. Academic Press, London.

Israelachvili, J. N. 1994. Strength of van der Waals attraction between lipid bilayers. *Langmuir*. 10:3369–3370.

Israelachvili, J. N., and H. Wennerström. 1992. Entropic force between amphiphilic surfaces in liquids. *J. Phys. Chem.* 96:520–531.

Janshoff, A., M. Neitzert, Y. Oberdörfer, and H. Fuchs. 2000. Force spectroscopy of molecular systems - single molecule spectroscopy of polymers and biomolecules. *Angew. Chem. Int. Ed.* 39:3212–3237.

Jenkins, A. T. A., T. Neumann, and A. Offenhäuser. 2001. Surface plasmon microscopy measurements of lipid vesicle adsorption on a micropatterned self-assembled monolayer. *Langmuir*. 17:265–267.

Johnson, K. L. 1985. Contact Mechanics. Cambridge University Press, Cambridge.

Künnecke, S., D. Krüger, and A. Janshoff. 2004. Scrutiny of the failure of lipid membranes as a function of headgroups, chain length, and lamellarity measured by scanning force microscopy. *Biophys. J.* 86: 1545–1553.

LeNeveu, D. M., R. P. Rand, and V. A. Parsegian. 1976. Measurement of forces between lecithin bilayers. *Nature*. 259:601–603.

LeNeveu, D. M., R. P. Rand, V. A. Parsegian, and D. Gingell. 1977. Measurement and modification of forces between lecithin bilayers. *Biophys. J.* 18:209–230.

Lis, L. J., M. McAlister, N. Fuller, R. P. Rand, and V. A. Parsesgian. 1982. Interactions between neutral phospholipid bilayer membranes. *Biophys. J.* 37:657–666.

Loi, S., G. X. Sun, V. Franz, and H.-J. Butt. 2002. Rupture of molecular thin films observed in atomic force microscopy. II. Experiment. *Phys. Rev. E.* 66:031602.

Maeda, N., T. J. Senden, and J. M. di Meglio. 2002. Micromanipulation of phospholipid bilayers by atomic force microscopy. *Biochim. Biophys. Acta*. 1564:165–172.

Marra, J., and J. Israelachvili. 1985. Direct measurement of forces between phosphatidylcholine and phosphatidylethanolamine bilayers in aqueous electrolyte solutions. *Biochemistry*. 24:4608–4618.

McDaniel, R. V., T. J. McIntosh, and S. A. Simon. 1983. Nonelectrolyte substitution for water in phosphatidylcholine bilayers. *Biochim. Biophys. Acta*. 731:97–108.

McIntosh, T. J., S. Advani, R. E. Burton, D. V. Zhelev, D. Needham, and S. A. Simon. 1995. Experimental tests for protrusion and undulation pressures in phospholipid bilayers. *Biochemistry*. 34:8520–8532.

Mueller, H., H.-J. Butt, and E. Bamberg. 2000. Adsorption of membrane associated proteins to lipid bilayers studied with an atomic force microscope: Myelin basic protein and cytochrome c. *J. Phys. Chem*. 104: 4552–4559.

Nir, S., and M. Andersen. 1977. Van der Waals interactions between cell surfaces. *J. Membr. Biol*. 31:1–18.

Parsegian, V. A., N. Fuller, and R. P. Rand. 1979. Measured work of deformation and repulsion between lecithin bilayers. *Proc. Natl. Acad. Sci. USA*. 76:2750–2754.

Persson, P. K. T., and B. A. Bergenstrahl. 1985. Repulsive force in lecithin gylcol lamellar phases. *Biophys. J*. 47:743–746.

Petrache, H. I., N. Gouliaev, S. Tristram-Nagle, R. Zhang, R. M. Suter, and J. F. Nagle. 1998. Interbilayer interactions from high-resolution x-ray scattering. *Phys. Rev. E*. 57:7014–7024.

Puu, G., and I. Gustafson. 1997. Planar lipid bilayers on solid supports from liposomes — factors of importance for kinetics and stability. *Biochim. Biophys. Acta*. 1327:149–161.

Rädler, J., H. Strey, and E. Sackmann. 1995. Phenomenology and kinetics of lipid bilayer spreading on hydrophilic surfaces. *Langmuir*. 11:4539–4548.

Richter, R. P., and A. Brisson. 2003. Characterization of lipid bilayers and protein assemblies supported on rough surfaces by atomic force microscopy. *Langmuir*. 19:1632–1640.

Sackmann, E., H. P. Duwe, and H. Engelhardt. 1986. Membrane bending elasticity and its role for shape fluctuations and shape transformations of cells and vesicles. *Faraday Discuss. Chem. Soc*. 81:281–290.

Schneider, J., W. Barger, and G. U. Lee. 2003. Nanometer scale surface properties of supported lipid bilayers measured with hydrophobic and hydrophilic atomic force microscope probes. *Langmuir*. 19:1899–1907.

Schneider, J., Y. F. Dufrene, W. R. Barger, and G. U. Lee. 2000. Atomic force microscope image contrast mechanisms on supported lipid bilayers. *Biophys. J*. 79:1107–1118.

Servuss, R. M., W. Harbich, and W. Helfrich. 1976. Measurement of the curvature-elastic modulus of egg lecithin bilayers. *Biochim. Biophys. Acta*. 436:900–903.

Sheetz, M. P. 2001. Cell control by membrane-cytoskeleton adhesion. *Nat. Rev. Molec. Cell Biol*. 2:392–396.

Sofou, S., and J. L. Thomas. 2003. Stable adhesion of phospholipid vesicles to modified gold surfaces. *Biosens. Bioelectron*. 18:445–455.

Stefani, G., F. Onofri, F. Valtorta, P. Greengard, and F. Benfenati. 1997. Kinetic analysis of the phosphorylation-dependent interactions of synapsin I with rat brain synaptic vesicles. *J. Physiol*. 504:501–515.

Visser, J. 1972. On Hamaker constants: A comparison between Hamaker constants and Lifshitz-van der Waals constants. *Adv. Colloid Interface Sci*. 3:331–363.